AXIAL STICK-SLIP LIMIT CYCLING IN DRILL-STRING DYNAMICS WITH DELAY

Christophe Germay
Department of Electrical Engineering and Computer Science
University of Liege
Belgium
christophe.germay@ulg.ac.be

Nathan van de Wouw
Department of Mechanical Engineering
Eindhoven University of Technology
Netherlands
n.v.d.wouw@tue.nl

Rodolphe Sepulchre
Department of Electrical Engineering and Computer Science
University of Liege
Belgium
R.Sepulchre@ulg.ac.be

Henk Nijmeijer
Department of Mechanical Engineering
Eindhoven University of Technology
Netherlands
h.nijmeijer@tue.nl

Abstract

In a novel approach to model stick-slip vibrations occurring when drilling with drag bits, the axial and torsional dynamics are coupled through the boundary conditions via a state-dependent delay. Moreover, friction is modelled by a rate-independent discontinuous term.

A regime characterized by a low amplitude of the torsional vibrations and a high drilling efficiency is numerically observed for some sets of parameters. In this regime, the axial fast vibrations have a stabilizing effect on the torsional equilibrium.

To understand this stabilizing mechanism, we are studying the decoupled axial equation obtained by freezing the delay. This approximation reflects the small variations of the delay when the bit experiences small torsional vibrations. Axial periodic solutions may be analysed independently. Particularities of this equation lie in the presence of a delayed term and a non-smooth non linearity.

In this paper, we apply different well-known methods to study the periodic orbits of the axial dynamics. The results and limitations of semi-analytical (Describing Functions Method) and numerical procedures (Finite Difference Method, Shooting Method) are exposed here. We use these numerical techniques to investigate some particular properties of the system, such as the dependency of period time with the delay.

Key words

Limit cycle; non-smooth delay differential equation; stick-slip.

1 Introduction

Self-excited vibrations are common phenomena observed in drilling systems used by oil industries. Most frequent models in the literature use a single DOF in torsion with a velocity weakening law at the bit/rock interface, as an intrinsic property of the bit/rock interaction (Brett, 1992; Challamel, 2000).

A novel approach with 2 DOF's in axial and torsion presented in (Richard *et al.*, 2004) exhibits similar behaviors although all parameters are rate independent (Detournay and Defourny, 1992). The apparent decrease of the friction coefficient is shown to be directly related to axial vibrations of the bit and more precisely to intermittent losses of frictional contact.

Because of the helicoidal motion of the bit, the cutting forces depend on a varying delayed axial position of the bit. This delay dependence is ultimately responsible for the coupling of the two modes of oscillations and for the existence of self-excited vibrations. Numerical simulations show that they may degenerate into stick-slip oscillations or bit bouncing for sets of parameters in accordance with quantities measured in real field operations (Richard *et al.*, 2004). Such extreme types of vibrations are at the origin of important bit or drillstring failures.

In the 2 DOF model, another regime, characterized by a low amplitude of the torsional vibrations and a high drilling efficiency, is numerically observed for some sets of parameters. In this regime, the fast axial vibrations have a stabilizing effect on the torsional equilibrium. In order to understand the stabilizing mechanism, we first study the axial equation with a fixed delay, an approximation averaging the small variations of the angular velocity of the bit. The approximated model becomes decoupled from the torsional equation.

Particularities of this equation lie in the delayed term and a non-smooth non linearity.

We present results and limitations of semi-analytical (Describing Function Method) and numerical procedures (Finite Difference Method, Shooting Method) used to characterize the limit cycling in this DDE with a non-smooth nonlinearity. Moreover, we will use the shooting method to investigate some particular properties of this system such as the evolution of the period time of the limit cycles with the delay.

In Section 2, we present the drilling model and some typical numerical results. We describe the anti-resonance regime and motivate the analysis of the axial dynamics with a fixed delay. In Section 3, we discuss some qualitative observations made on this particular equation, the results and limitations of the different methods applied to analyze the periodic orbits. Conclusions are drawn in Section 5.

2 Drilling Model

The model of the drillstring consists in an angular pendulum of stiffness C ended with a punctual inertia I and a punctual mass M free to move axially (see Fig. $1(a)$). The boundary conditions applied to that mechanical system are: (i) at the top, a constant upward force H_o and a constant angular velocity Ω_o and (ii) at the bottom, bit/rock interactions laws based on a phenomenological model accounting for cutting and a rate-independent frictional processes (Detournay and Defourny, 1992).

During a slip phase (angular velocity of the bit is positive), the equations of motion of the drill bit are given by

$$I\frac{\mathrm{d}^2\Phi}{\mathrm{d}t^2} + C\left(\Phi - \Omega_\mathrm{o} t\right) = -T, \tag{1}$$

$$M\frac{\mathrm{d}^2 U}{\mathrm{d}t^2} = W_\mathrm{o} - W, \tag{2}$$

where U and Φ are the vertical and angular positions of the drag bit, respectively. The quantity W_o represents the effective weight transmitted to the drag bit by the drilling structure. Its amplitude is controlled by the hook force H_o.

For the sake of simplicity, the idealized drag bit considered here consists of n identical radial blades regularly spaced by an angle equal to $2\pi/n$, see Fig. $1(b)$. The weight and the torque required by the cutting action, W and T respectively, account for both independent cutting and frictional processes

$$T = T_\mathrm{c} + T_\mathrm{f} \tag{3}$$

$$W = W_\mathrm{c} + W_\mathrm{f}, \tag{4}$$

denoted respectively by the subscripts $_\mathrm{c}$ and $_\mathrm{f}$.

The rate independent frictional process is mobilized at the wears/rock contacts only when the bit is moving downward $\frac{\mathrm{d}U}{\mathrm{d}t} \geq 0$. Otherwise, the frictional contacts vanish. The pure cutting forces are, among other things, proportional to the rock thickness d_n that is removed instantaneously. When the bit experiences axial vibrations, the rock ridge facing the blades may vary. Because of the helicoidal motion (the bottom hole profile was dictated by the passage of the previous blade), it brings into the equations the delayed axial position of the bit

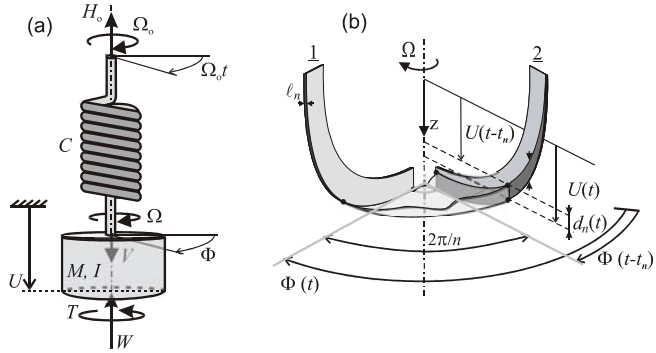

Figure 1. (a) Simplified model of a drilling system; (b) section of the bottom-hole profile located between two successive blades of a drill bit.

$$T_\mathrm{c}(t) \propto d_n(t) = U(t) - U(t - t_n), \tag{5}$$

$$W_\mathrm{c}(t) \propto d_n(t) = U(t) - U(t - t_n). \tag{6}$$

The delay t_n is the time required for the bit to rotate by an angle of $2\pi/n$ to reach its current angular position. If the bit experiences torsional vibrations, the delay is not constant. It is the solution of

$$\int_{t-t_n}^{t} \frac{\mathrm{d}\Phi}{\mathrm{d}t}\mathrm{d}t = \Phi(t) - \Phi(t - t_n) = \frac{2\pi}{n}. \tag{7}$$

A conceptual sketch is depicted in Fig. $1(b)$. Because of the torsional vibrations, the bit angular velocity may fall to zero. Then, it enters a stick phase during which the bit is considered to be stuck. Since the top is still rotating, the elastic energy builds up in the spring until it becomes sufficient to provide a positive acceleration. The bit starts rotating again.

The expression of the dimensionless and perturbed form of the equations governing the bit motion of this discrete model during slip phase yields

$$\ddot{u} = \psi n\left(-v_\mathrm{o}\left(\tau_n - \tau_{n\mathrm{o}}\right) - \left(u - \tilde{u}\right) + g(\dot{u})\right) \tag{8}$$

$$\ddot{\varphi} = n\left(-v_\mathrm{o}\left(\tau_n - \tau_{n\mathrm{o}}\right) - \left(u - \tilde{u}\right)\right) + n\beta g(\dot{u}) - \varphi \tag{9}$$

$$0 = \omega_\mathrm{o}\left(\tau_n - \tau_{n\mathrm{o}}\right) + \varphi - \tilde{\varphi}, \tag{10}$$

where $u(\tau)$ and $\varphi(\tau)$ represent, respectively, the dimensionless perturbed axial and angular positions to

the trivial bit motion while the dot denotes differentiation with respect to the dimensionless time $\tau = t/\sqrt{I/C}$. The variables $\tilde{u} = u(\tau - \tau_n)$ and $\tilde{\varphi} = \varphi(\tau - \tau_n)$ correspond to delayed axial and angular positions, respectively.

The boundary conditions complicate significantly the model since the set of equations is non-linear and fully coupled with a state-dependent delay. Indeed, the solution of the axial equation (8) is exciting the torsional mode of vibrations (9). The state-dependent delay, which is the solution of the implicit torsional equation (10), affects the axial equation through the terms related to the pure cutting process. Finally, the friction process, represented by $g(\dot{u})$, is responsible for the presence of a discontinuous term in both equations that depends on the sign of the axial velocity. The discontinuous function that represents the frictional contacts occurring at the wears/rock interface yields

$$g(\dot{u}) = \frac{\lambda_n}{2}\left(1 - sign(\dot{u} + v_o)\right). \tag{11}$$

Rate independent dimensionless parameters of the model are:

(i) The quantities ω_o and v_o are the trivial angular and axial bit velocity, respectively.
(ii) The parameter β characterizes the geometry of the bit.
(iii) The number λ_n is proportional to the lengths of the wears. It is a direct measure of the bluntness of the bit.
(iv) The drill string design is embedded into the lumped parameter ψ.
(v) The trivial dimensionless delay is $\tau_{no} = 2\pi/n\omega_o$.

The typical range of variation of both parameters ω_o and v_o is $[1, 10]$. The bluntness number λ_n is of order 1, while the bit-rock interaction number β is typically within the interval $[0.1, 1]$. The parameter ψ is large in the range $\left[10^2, 10^3\right]$.

The term $-v_o(\tau_n - \tau_{no}) - u + \tilde{u}$ represents the perturbed thickness of rock that is cut instantaneously by each blade. In absence of any torsional vibrations

$$\tau_n = \tau_{no}, \tag{12}$$

while in absence of any axial vibrations

$$u = \tilde{u} = 0. \tag{13}$$

The solutions of the discontinuous differential equation are defined using Filippov's solution concept. Filippov's convex method treats the discontinuous term in the right-hand side of (8) and (9) as a set-valued mapping on the hyperplane $\dot{u} = -v_o$. The magnitude of ψ will separate the dynamics associated to both equations (8) and (9). Indeed, we can roughly conclude that the axial dynamics will evolve $\sqrt{\psi}$ faster than the dynamics related to the torsional equation.

The numerical simulations reveal different regimes such as:

1. **The stick-slip vibrations** are characterized by large amplitude torsional vibrations. Dominant frequencies in both modes differ strongly. The dominant frequency in torsion is directly related to the characteristic time of the torsional oscillator ($\sqrt{C/I}$) while axial dominant frequency is clearly larger. Stick-slip vibrations are undesired because they are the most frequent cause of drillstring breakage by fatigue.
2. **The anti-resonance regime** is characterized by small oscillations of $\dot{\varphi}$ around the steady-state value. The dominant frequency in both modes coincides and is larger than the natural frequency of the drillstring in torsion. It occurs mainly at low RPM (ω_o).

2.1 Anti-resonance mode

For some sets of parameters, the limit cycle of the torsional vibrations is characterized by small variations of the bit angular velocity around its steady state value. The natural frequency of the torsional mode has disappeared to make place for high frequency oscillations. These vibrations are directly linked to the axial dynamics that remain clearly observable (see Fig. 2). The two time scales are also clearly visible during the transient. The variables related to torsion evolve with a characteristic time of 2π while the axial oscillations have a period close to 1.

As said above, this regime is particularly interesting since it should reduce considerably the risks of failure by fatigue of the drill string.

In the anti-resonance mode, numerical observations show that the variable $\dot{u}$ is periodic. Therefore, the mean value of $\ddot{u}$ on a period time, denoted $\langle \ddot{u} \rangle$ is zero and the position u can be written as the superposition of a periodic signal u^p of zero mean and linear growth with time

$$u = u^p + \langle \dot{u} \rangle \tau \tag{14}$$

However, the variable $u - \tilde{u}$ is purely periodic but of mean value equal to $\langle g(\dot{u}) \rangle$.

Therefore, we introduce a new set of variables $x_1 = u - \tilde{u}, x_2 = \dot{u}, x_3 = \varphi$ and $x_4 = \dot{\varphi}$. After some ma-

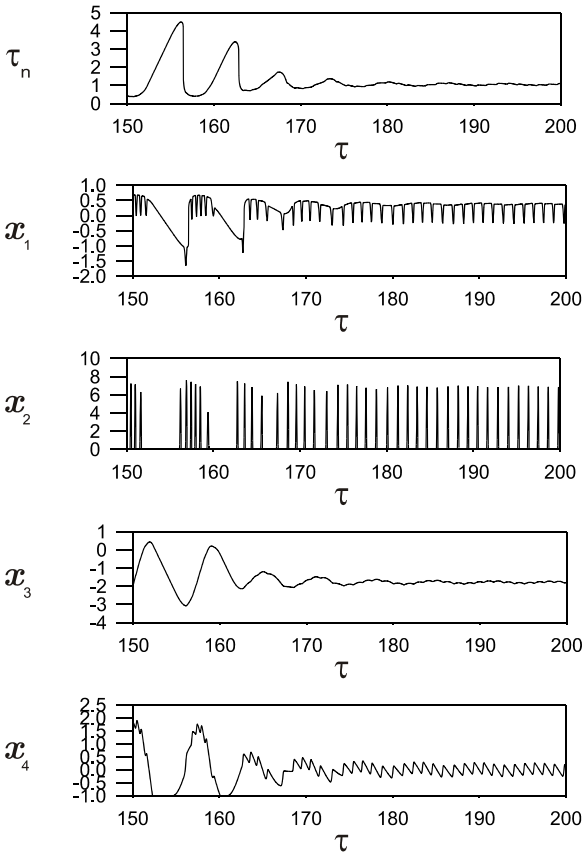

Figure 2. Anti-resonance Regime.

nipulations, we can rewrite (8), (9) and (10) as follow:

$$\dot{x}_1 = x_2 - \tilde{x}_2 \tag{15}$$
$$\dot{x}_2 = \psi n \left(-v_o \left(\tau_n - \tau_{no}\right) - x_1 + g(x_2)\right) \tag{16}$$
$$\dot{x}_3 = x_4 \tag{17}$$
$$\dot{x}_4 = -x_3 + n\left(\beta - 1\right)\left[v_o\left(\tau_n - \tau_{no}\right) + x_1\right] + \frac{\beta}{\psi}\dot{x}_2 \tag{18}$$
$$\tau_n = -\frac{x_3 - \tilde{x}_3}{\omega_o} + \tau_{no}. \tag{19}$$

We must emphasize that the solution of (8) is only a particular solution of formulation (15) and (16). Indeed, we suppress one internal constrain of the system when derivating $x_1 = u - \tilde{u}$ to obtain (15). In that respect, by using relation (14), we can write that

$$x_1 = u^p - \tilde{u}^p + \langle \dot{u} \rangle \tau_n \tag{20}$$
$$x_2 = \dot{u}^p + \langle \dot{u} \rangle . \tag{21}$$

Therefore, the integration of (15) when considering (21) gives

$$\begin{aligned} x_1 &= \int_0^{\tau} \dot{u}^p(t)\mathrm{dt} - \int_{-\tau_n}^{\tau-\tau_n} \dot{u}^p \mathrm{dt} \\ &= u^p - \tilde{u}^p + C, \end{aligned} \tag{22}$$

where C is a constant that depends on the initial conditions. Therefore, the solution of (8) is only a particular solution of (15) and (16) when $C = \langle \dot{u} \rangle \tau_n$.

By assuming small variations of the angular position and velocity around the equilibrium point, we can linearize (19) around its trivial value

$$\tau_n \approx \frac{2\pi}{n\left(\omega_o + x_4\right)} = \tau_{no} - \frac{2\pi}{n\omega_o^2} x_4. \tag{23}$$

Substituting (23) in (17) and (18), we obtain

$$\dot{x}_3 = x_4 \tag{24}$$
$$\dot{x}_4 = -x_3 - \left(\beta - 1\right)\frac{v_o 2\pi}{\omega_o^2} x_4 + n\left(\beta - 1\right) x_1 + \frac{\beta}{\psi}\dot{x}_2 \tag{25}$$
$$\tau_n = -\frac{x_3 - \tilde{x}_3}{\omega_o} + \tau_{no}. \tag{26}$$

It is therefore the coupling between the torsional dynamics and the axial dynamics that has a stabilizing effect on the torsional equilibrium. To simplify the analysis, we exploit the time scales separation (Strogatz, 1994) between the "fast" axial dynamics and the "slow" torsional dynamics. The "fast" axial dynamics is decoupled from the torsional dynamics by treating the delay as a fixed parameter. In the rest of the paper, we focus on this simplified axial equation, postponing the analysis of the slow dynamics to a future work.

3 Decoupled Axial Equation

Equations (15) and (16) with a fixed delay can be rewritten as

$$\mathring{w}_1 = \tilde{w}_2 - w_2 \tag{27}$$
$$\mathring{w}_2 = w_1 + \bar{g}(w_2) \tag{28}$$

where $w_1 = -x_1\left(\bar{\tau}\right)$ and $w_2 = x_2\left(\bar{\tau}\right)/\sqrt{n\psi}$ with $\bar{\tau} = \tau\sqrt{n\psi}$, $\bar{\tau}_{no} = 2\pi\sqrt{n\psi}/n\omega_o$, $\bar{g}(w_2) = \frac{\lambda_n}{2}\left(1 - sign\left(w_2 + \bar{v}_o\right)\right)$ and $\bar{v}_o = v_o/\sqrt{n\psi}$. The round dot denotes differentiation with respect to the time $\bar{\tau}$. Initial conditions required to solve this system consist of

$$\begin{cases} w_1(0) \\ w_2(\bar{\tau}) \end{cases} \quad \text{for } \bar{\tau} \in [-\bar{\tau}_{no}, 0] \tag{29}$$

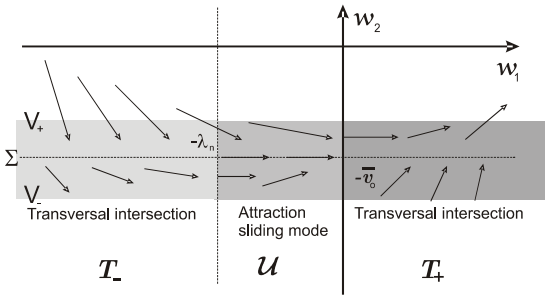

Figure 3. Different modes of the vector field in the vincinity of the hyperplane Σ when $\tilde{w}_2 > -v_o$.

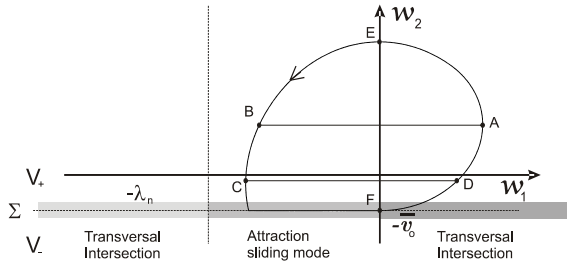

Figure 4. Sketch of a typical limit cycle in the space w_1, w_2.

System (27-28) is infinite dimensional because of the delay and it contains a discontinuous function.

The equilibrium point is the trivial solution $w_1 = w_2 = 0$. It can be shown that the poles of the transfer function of this system are purely imaginary when $\bar{\tau}_{no} = (2k+1)\,\pi/\sqrt{2},\ k \in \mathbb{N}$. Numerical simulations confirm that the equilibrium point is asymptotically stable for $\bar{\tau}_{no} < \pi/\sqrt{2}$, marginally stable when $\bar{\tau}_{no} = \pi/\sqrt{2}$ and unstable otherwise.

In the last case, the system evolves towards a stable limit cycle for $\bar{\tau}_{no} < \bar{\tau}^*_{no}$ that depends on the parameters of the system. Otherwise, the amplitude of the solutions grows without bound as $t \to \infty$.

3.1 Qualitative analysis of the limit cycle in the state space

Let us define the subspace V_+ (V_-) as the semi-infinite plane in the state space such that $w_2 > -\bar{v}_o$ ($w_2 < -\bar{v}_o$). Focusing on the vicinity of Σ (hyperplane $w_2 = -\bar{v}_o$), we can directly define three different zones:

1. T_-; $w_1 < -\lambda_n$, the vector field is pushing the solution from V_+ into the subspace V_- (Transversal Intersection I)
2. $\mathcal{U}$; $0 > w_1 > -\lambda_n$, the vector field in each subspace drives the solution toward the hyperplane Σ (Attraction sliding mode)
3. T_+; $w_1 > 0$, the vector field is pushing the solution from V_- in the subspace V_+ (Transversal intersection II)

These three zones and the vector field are depicted into the Fig. 3.

In Figure 4, a typical periodic solution is depicted. Note that the space (w_1, w_2) is not the state space, which is infinite dimensional due to the delay $\bar{\tau}_{no}$. In that figure, particular points of the limit cycle are shown. Points A and C are characterized by $\mathrm{d}w_1/\mathrm{d}w_2 = 0$. Therefore, it yields that $w_2(\bar{\tau}) = w_2(\bar{\tau} - \bar{\tau}_{no})$. The delay $\bar{\tau}_{no}$ is therefore the time elapsed to cover the trajectory from state position B to state position A, and from D to C, respectively. It can not be a transition from point A to A since the delay is always less than the period of the limit cycle (see section 3.2.3).

The limit cycle will always leave the stick phase when w_1 becomes equal to 0 since it enters the subspace (V_+, T_+) characterized by $\bar{g}(w_2) = 0$.

Now that we have a qualitative understanding of the limit cycle, we proposed to use well-known semi-analytical or numerical methods to determine the limit cycle and stability properties more precisely while changing the delay since it varies slowly in the solution of the complete model.

3.2 Semi-analytical and numerical methods

Several methods exist to analyze the limit cycles of nonlinear dynamical systems. The describing function method and two numerical methods (finite difference method and the shooting method) are applied to the problem at hand. The results obtained by application of these methods and their limitations while applying it to a discontinuous delay differential equation as (27) and (28) are discussed below.

3.2.1 Describing Function Methods The general idea of the describing function method is to use the Fourier series property that says that any periodic signal can be represented as the sum (finite or infinite) of distinct harmonic functions (Khalil, 1996). One has to identify a minimum number of coefficients of this Fourier series in order to obtain a good estimate of the real limit cycle. In the case where only few harmonics (ideally one) are sufficient to describe the limit cycle, this tool may be efficient. It provides an estimate of the dominant frequency ω_s, an estimate of the amplitude of the vibrations a and an estimate of the mean value of the vibrations $\hat{a}_o$.

Here, the estimation ω_s of the frequency of the periodic orbit is matching the dominant frequency of the signal obtained when integrating the equation of motion. However, contradictions occurred when evaluating $\hat{a}_o$ and a. For some set of parameters $(\bar{\tau}_{no}, \lambda_n, \bar{v}_o)$, no solutions for a exists although limit cycle was clearly observed when integrating numerically. These issues are probably due to the lack of the stick phase when using only the first mode of the Fourier series. Clearly, higher harmonics are needed to describe a stick-slip limit cycle as in Fig. 4.

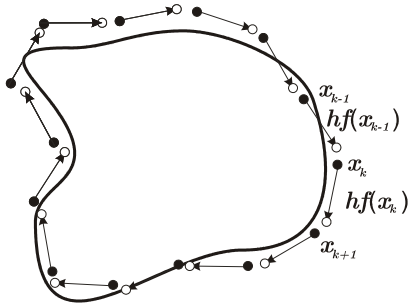

Figure 5. Sketch of the Finite Difference Method. $\mathbf{f}(\mathbf{x})$ is the vector field in the state space while h is the time step chosen in the numerical method.

3.2.2 Finite Difference Method The finite difference method approximates the periodic limit cycle with linear segments that are in the direction of the vector field (see Fig. 5). An algebraic system of equations is then derived. Solutions gives increments of the node positions to converge towards the periodic orbit. This method is recognized to have a fast convergence and large basins of attraction but it can only be applied to smooth systems (**?**).

Therefore, one must smoothen the discontinuity using for example

$$\bar{g}(w_2) \approx \frac{\lambda_n}{2}\left(1 - \frac{2}{\pi}\mathrm{Arc}\tan\left(\epsilon\left(w_2 + \bar{v}_\mathrm{o}\right)\right)\right) \quad (30)$$

with ϵ large. However, the equations become stiff requiring a large number of nodes to obtain a good estimate.

Furthermore, the resolution of the algebraic system remains always singular whatever the set of parameters considered. As we will see later, it can possibly be explained by the existence of a continuum of limit cycles due to the change of variable done before that ultimately removes an internal constrain.

3.2.3 Shooting Method The shooting method aims to find initial conditions belonging to the limit cycle by solving a two-point boundary-value problem (see Fig.6). On top of that, this method also provides Floquet's multipliers that give information on the stability of the limit cycle. In principle, this method can easily deal with discontinuous differential equations (**?**).

If an initial state $\mathbf{x}_\mathrm{o} = \mathbf{x}(\bar{\tau}_\mathrm{o})$ belongs to a periodic solution of period T, we can obviously write

$$\mathbf{H}(\mathbf{x}_\mathrm{o}, T) \equiv \mathbf{x}_T - \mathbf{x}_\mathrm{o} = 0, \quad (31)$$

where $\mathbf{x}_T = \mathbf{x}(\bar{\tau}_\mathrm{o} + T)$. Therefore, this two-point boundary-value problem is solved when a zero of $\mathbf{H}(\mathbf{x}_\mathrm{o}, T)$ is found. By using a Newton-Raphson procedure and after the evaluation of the partial derivative,

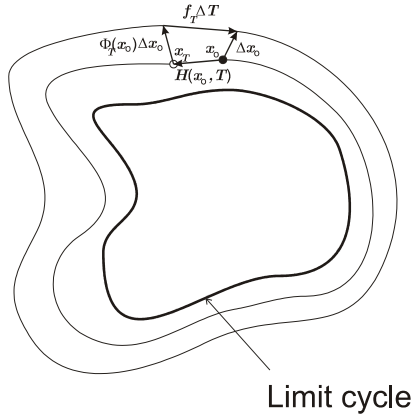

Figure 6. Graphical representation of the shooting method.

the set of equations to solve yields

$$\left(\mathbf{\Phi}_T(\mathbf{x}_\mathrm{o}) - \mathbf{I}\right)\Delta\mathbf{x}_\mathrm{o} + \mathbf{f}\left(\mathbf{x}_T\right)\Delta T = \mathbf{x}_\mathrm{o} - \mathbf{x}_T, \quad (32)$$

where $\mathbf{\Phi}_T(\mathbf{x}_\mathrm{o})$ is the monodromy matrix and $\mathbf{f}(\mathbf{x})$ is the vector field in the state space. The stability property of periodic solutions can be derived from the knowledge of $\mathbf{\Phi}_T(\mathbf{x}_\mathrm{o})$. The periodic solutions will be asymptotically stable if all the eigenvalues of the monodromy matrix (called Floquet's multipliers) lie within the unit circle in the complex plane, except one which must be equal to 1 for autonomous systems. It corresponds to the perturbation along the periodic orbit.

Referred to as *anchor equation*, one additional equation will be provided to define uniquely the solution of the system. Its choice is more or less arbitrary. One possibility consists in fixing one coordinate of one of the nodes if the periodic solution is shown to have at least one intersection with the hyperplane Σ. Alternatively, orthogonality conditions can be imposed to ensure that the increment $\Delta\mathbf{x}_j$ is transversal to the vector field.

The application to DDE's is particular since the initial condition is infinite dimensional. In order to apply the shooting method, we first discretize the initial condition over the delay interval

$$\mathbf{x}_{\mathrm{o},i} = \mathbf{x}(\bar{\tau}_\mathrm{o} - \bar{\tau}_{n\mathrm{o}} + ih) \quad (33)$$

for $i = 0, ..., m$ and m is defined as $m = \bar{\tau}_{n\mathrm{o}}/h$. Since the delay appears only in the second state variable, the number of initial conditions needed will be $m + 1$ (m for w_2 and 1 for w_1).

This method is time consuming when applied to DDE's since $m + 1$ equations must be integrated at each time step to obtain a numerical estimate of the monodromy matrix.

One other drawback of this method is in the guess of the initial conditions on the limit cycle and the choice of the anchor condition. The presence of a stick phase

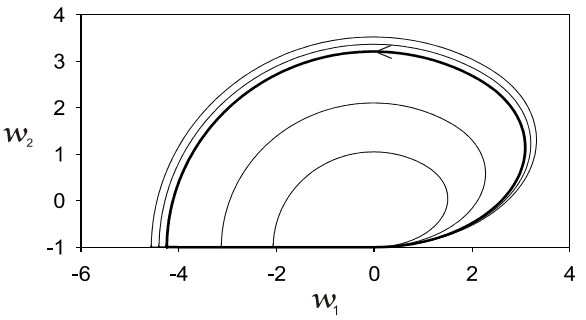

Figure 7. Coexistence of different limit cycles.

and the non-smooth adhesion of the trajectory on the hyperplane Σ strongly increases the sensitivity of the convergence of the method on the initial conditions and the anchor condition. Only certain combinations of them ensure convergence of the method. For example, it was often observed that if a part of the initial conditions contains a part of the hyper surface Σ, the method may be completely inefficient. This situation is always encountered for large delays.

This issue is clearly a consequence of the discontinuous vector field and the existence of the stick phase. Hence, to regularize the problem, the switch model was implemented.

The switch model is a numerical technique used to integrate numerically discontinuous differential equations (Leine and Nijmeijer, 2004) with a small number of switching planes. This method is an improved version of the Karnop model which introduces a stick band ($|v_{rel}| < \eta$) that approximates the stick mode. With the switch model, the trajectories are pushed to the middle of the stick band, avoiding numerical instabilities.

If the hyper surface Σ is analytically defined by the locus of points satisfying $h(\mathbf{x}) = 0$, then exponential convergence towards the hyper surface in the attractive $\mathcal{U}$ sliding mode is forced by setting

$$\dot{h} = -\tau^{-1} h,$$

which will force $h \to 0$ with the time constant τ.

3.3 Numerical Results

Numerical results indicate that several limit cycles coexist for the same set of parameters. As an example, Figure 7 shows several limit cycles for an identical set of parameters ($\bar{\tau}_{no} = 4.5$, $\bar{v}_o = 1$ and $\lambda_n = 10$) but different initial conditions. For one of this limit cycle, typical location of the Floquet's multipliers in the complex plane is shown in figure 8. Particular attention is paid to the presence of a second multiplier located at $(1, 0)$. Approximately all the others are located close to the origin. It is a direct consequence of the discontinuity in the system. Similar patterns seem to be reproduced when zooming in. The second multiplier at

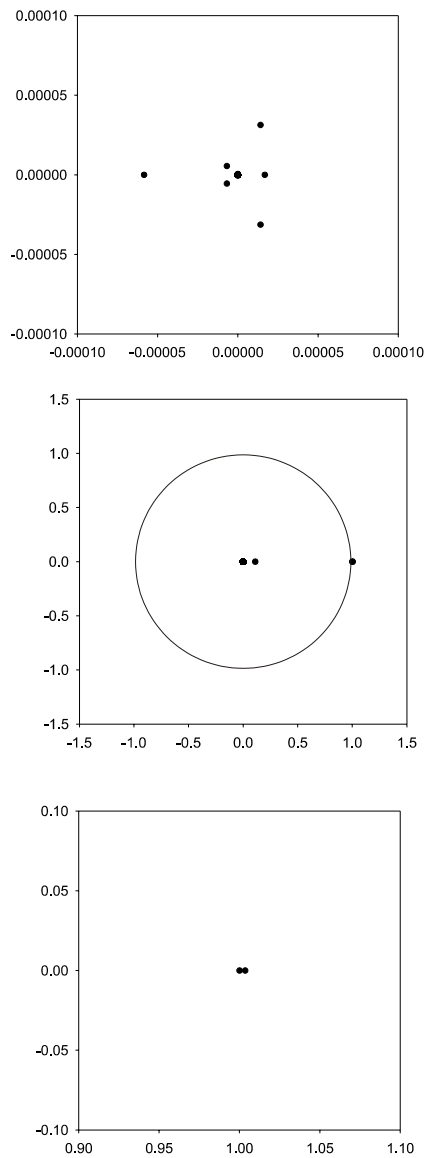

Figure 8. Layout of the Floquet's multipliers in the complex plane when $\bar{\tau}_{no} = 4.5$, $\bar{v}_o = 1$ and $\lambda_n = 10$.

1 could be explained by the existence of a continuum of limit cycles, which means that the infinite number of periodic orbits infinitely close to each other could coexist. However, that explanation has not yet been proved rigorously. In this respect, we stress the fact that in Figure 7 we depicted limit cycles in a two-dimensional plot even though they belong to an infinite dimensional state-space.

In Figure 9, we plotted the evolution of periods of 5 different limit cycles with the delay that are obtained with the same set of parameters but from 5 different initial conditions. The periods are identical whatever the amplitude of the periodic orbit considered. Moreover, the period time seems to vary linearly with the delay $\bar{\tau}_{no}$ with a coefficient of proportionality equal to 1.

The miss of an internal constrain when doing the

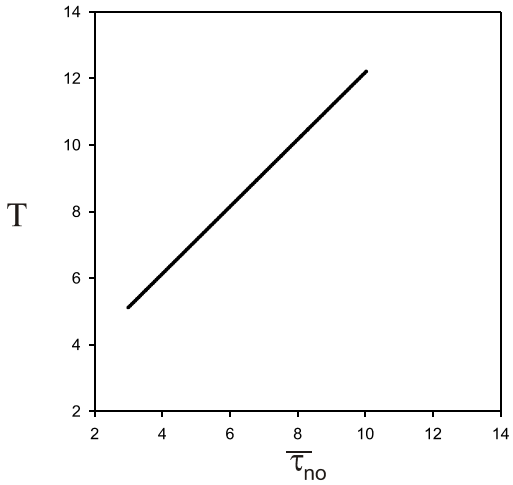

Figure 9. Evolution of the period time of 5 different limit cycles obtained with 5 different initial conditions with respect to the delay.

change of variable $x_1 = u - \tilde{u}$ is responsible for the coexistence of the infinite number of periodic solutions. By imposing that the initial condition must satisfy

$$w_1 = -\int_{-\bar{\tau}_{no}}^{0} w_2(t)\mathrm{dt}, \tag{34}$$

the size of the algebraic system that must be solved is reduced by one. The numerical results obtained with the shooting method exhibit only one limit cycle, the solution of (8) when the delay is fixed and equal to τ_{no}. It is represented in Fig. 7 by the trajectory with the narrow. The correpsonding Floquet's multipliers are again all located close to the origin, but in this case only one remain equal to 1.

4 Conclusions

A novel approach to model stick-slip vibrations of drag bit in drilling structure accounts for coupled axial and torsional modes of vibrations via the bit/rock interface laws. These boundary conditions bring into the equations of motion a state-dependent delay and a discontinuous term due to friction. A dimensionless formulation shows that the large parameter ψ in the axial equation of motion generates two different time scales.

Numerical simulations show existence of stick-slip vibrations and an anti-resonance regime that is characterized by small and fast torsional vibrations, following the axial dynamics. Ultimately, we want to understand the mechanisms responsible for the stabilization of the torsional mode. In this context, a two-timing approach and the small variations of the delay suggest that the latter can be frozen in the axial equation. This approximation decouples the axial equation from the torsional vibrations.

Different well-known methods to find a periodic orbit and its characteristics are applied to the differential equation with a fixed delay and a discontinuity.

The Describing Function Method is partly inefficient when applied to this equation. We obtain a good estimate for the dominant frequency but the mean value and the amplitude of the dominant vibrations were badly estimated. This issue can be explained by the importance of higher harmonics in the power spectrum of the axial stick-slip limit cycle that are not captured by the first mode of vibrations.

The Finite difference method is only applicable to smooth systems. After smoothing the discontinuity, the algebraic system derived to obtain an increment of node positions was always singular due to the change of variable done to obtain a periodic orbit in (x_1, x_2) and moreover extremely large.

The shooting method, which can deal with non-smooth equations, is implemented. This method gives satisfactory results for small delays. Nevertheless, for larger delays, it encounters issues for converging towards the limit cycle. It is clearly identified that the non-smooth part of the solution when entering the sliding mode is the cause of this problem. By using the switch model, we can regularize that issue and obtain solutions for arbitrary sets of parameters.

With that method, numerical simulations reveal the coexistence of several periodic orbits for identical sets of parameters but different initial conditions. All are characterized by identical periods that vary linearly with the delay. Moreover, a second Floquet's multipliers is equal to 1. The existence of a continuum of limit cycles is a plausible explanation of the second multiplier at 1 and the issues of singularities encountered in the Finite Difference Method. However, this particularity can easily be suppressed in the shooting method by imposing a constrain on the initial conditions. Therefore, the solution obtained with the shooting method becomes unique and converge toward the equivalent solution of the initial problem with a fixed delay.

These results, such as the evolution of the period time with the delay, will be exploited in the complete model to understand the stabilizing effect of the fast axial vibrations on the slow torsional oscillations.

5 Acknowledgements

This work is the result of an internship of three months made at the TU/e in the framework of a First Europe Project. The first author really appreciated to meet so welcoming and warm people that belong to the DCT group and looks forward to meet them again. This paper presents research partially supported by the Belgian Programme on Inter-university Poles of Attraction, initiated by the Belgian State, Prime Minister's Oce for Science, Technology and Culture.

References

Brett, J. F. (1992). The genesis of torsional drillstring vibrations. *SPE Drilling Engineering* pp. 168–174.

Challamel, N. (2000). Rock destruction effect on the stability of a drilling structure. *Journal of Sound and Vibration* **233**(2), 235–254.

Detournay, E. and P. Defourny (1992). A phenomenological model of the drilling action of drag bits. *Int. J. Rock Mech. Min. Sci. & Geomech. Abstr.* **29**(1), 13–23.

Khalil, H. K. (1996). *Nonlinear Systems*. 2nd ed.. Prentice Hall.

Leine, R. I. and H. Nijmeijer (2004). *Dynamics and Bifurcations of Non-Smooth Mechanical Systems*. Springer Verlag Berlin Heidelberg New York.

Richard, T., C. Germay and E. Detournay (2004). Self-excited stick-slip oscillations of drill bits. *C. R. Mecanique* **332**, 619–626.

Strogatz, S. H. (1994). *Nonlinear Dynamics and Chaos*. Perseus Books.